

Optical force between two coupled identical parallel optical nanofibers

Fam Le Kien ¹, Síle Nic Chormaic ^{1,2} and Thomas Busch ¹

¹Okinawa Institute of Science and Technology Graduate University, Onna, Okinawa 904-0495, Japan

²Laboratoire de Physique des Gaz et des Plasmas, CNRS, Université Paris-Saclay, 91405 Orsay, France



(Received 3 March 2022; accepted 15 June 2022; published 27 June 2022)

We study the optical force between two coupled parallel identical nanofibers using the rigorous array mode theory. We numerically demonstrate for the coupled nanofibers that the forces of the even array modes are attractive, while the forces of the odd array modes are repulsive. We examine the dependencies of the optical forces on the array mode type, the fiber radius, the light wavelength, and the fiber separation distance. We show that for a given power and a given separation distance, the absolute value of the force achieves a peak when the fiber radius and the light wavelength are appropriate.

DOI: [10.1103/PhysRevA.105.063517](https://doi.org/10.1103/PhysRevA.105.063517)

I. INTRODUCTION

Two coupled waveguides are essential components of several optical devices such as optical directional couplers, multicore fibers, polarization splitters, interferometers, and ring resonators [1–3]. It is known that the overlap of the modes of evanescently coupled waveguides or cavities results in an optical gradient force [4–9], and examples of devices where this is exploited include coupled strip waveguides [4], a waveguide suspended over a silica substrate [8], coupled slab waveguides [9], coupled whispering-gallery-mode microspheres [10,11], coupled guiding mirrors [12], and coupled microring resonators [13]. It has already been shown that the optical gradient force between two coupled dielectric structures is attractive or repulsive depending on whether a symmetric or antisymmetric mode is excited [4–13]. The optical gradient forces between coupled macroscopic structures have been experimentally observed for a waveguide coupled to a high- Q microresonator [14] or to a dielectric substrate [15], coupled nanophotonic waveguides [16,17], and coupled ring resonators [18].

Optical devices based on coupled tapered thin fibers have been produced and studied [19–21]. Recently, miniaturized optical devices composed of coupled twisted and knotted optical nanofibers have been fabricated [20]. The optical nanofibers have a subwavelength diameter and significantly different core and cladding refractive indices [22]. Such ultrathin fibers allow for a guided light field, which has tight radial confinement, to propagate along the fiber for a long distance and to interact efficiently with nearby emitters, absorbers, and scatterers [23–25].

Coupling between two optical nanofibers has been studied in the framework of the coupled mode theory [20,26]. A rigorous theory for the guided normal modes of two coupled dielectric rods has been developed using the circular harmonics expansion method [27]. This theory has been extended to multicore fibers [28–31] and has been used to study the propagation constant [27,31,32], the flux density [27], the polarization pattern [31], the mode cutoff [33], the spatial field intensity distributions [34], and the atom trapping [35]. The photon coupling efficiency of a twin-nanofiber structure has recently been investigated by numerical simulations based on the finite-difference time-domain method [36].

In this work, we study the optical force between two coupled identical parallel optical nanofibers. We show that the forces are attractive for even array modes and repulsive for odd array modes. We examine the dependencies of the optical forces on the array mode type, the fiber radius, the light wavelength, and the fiber separation distance.

The paper is organized as follows. In Sec. II, we present the model for the system of two coupled identical parallel optical nanofibers and review the calculation methods for the optical forces between the waveguides. In Sec. III, we calculate numerically the optical force between the nanofibers. Finally, we conclude in Sec. IV.

II. TWO COUPLED IDENTICAL PARALLEL OPTICAL NANOFIBERS

A. Model and array modes

We study two identical vacuum-clad, optical nanofibers that lie parallel to each other along the direction of the fiber axis (see Fig. 1). The fibers are labeled by the indices $j = 1, 2$. Each nanofiber j can be viewed as a dielectric cylinder with a radius a and a refractive index $n_f > 1$, surrounded by an infinite background of vacuum or air with a refractive index $n_0 = 1$. The diameter of each nanofiber is taken to be a few hundreds of nanometers and each can support either a single or multiple modes depending on the fiber size parameter

Published by the American Physical Society under the terms of the [Creative Commons Attribution 4.0 International license](https://creativecommons.org/licenses/by/4.0/). Further distribution of this work must maintain attribution to the author(s) and the published article's title, journal citation, and DOI.

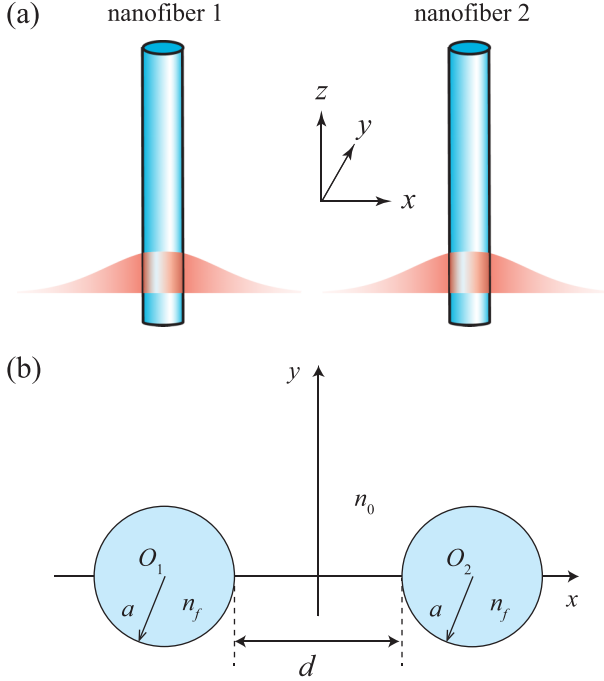


FIG. 1. (a) Two coupled parallel optical nanofibers and (b) the geometry of the system.

$V = ka\sqrt{n_f^2 - n_0^2}$. Here, $k = \omega/c$ is the wave number of light with an optical frequency ω in free space.

We introduce the global Cartesian coordinate system $\{x, y, z\}$, where z is parallel to the z_1 and z_2 axes of the fibers, x is perpendicular to the z axis and connects the centers O_1 and O_2 of the fibers, and y is perpendicular to the x and z axes (see Fig. 1). The plane xy is the transverse (cross-sectional) plane of the fibers. The positions of the fiber centers O_1 and O_2 along x are taken to be $O_1 = -(a + d/2)$ and $O_2 = a + d/2$, where d is the separation distance between the two fibers.

The normal modes of the coupled fibers are termed array modes. We study the array modes of a light field with an optical frequency ω which propagates in the $+z$ direction with a propagation constant β . The electric and magnetic components of the field can be written as $\mathbf{E} = [\mathcal{E}e^{-i(\omega t - \beta z)} + \text{c.c.}]/2$ and $\mathbf{H} = [\mathcal{H}e^{-i(\omega t - \beta z)} + \text{c.c.}]/2$, respectively, where \mathcal{E} and \mathcal{H} are the slowly varying complex envelopes.

The rigorous theory for the guided normal modes of two parallel dielectric cylinders has been formulated in Ref. [27]. The results of this theory have been summarized and discussed in detail in Ref. [34]. According to Refs. [27,34], two coupled identical parallel fibers have four types of guided normal modes, namely, the even \mathcal{E}_z -cosine modes, the odd \mathcal{E}_z -cosine modes, the even \mathcal{E}_z -sine modes, and the odd \mathcal{E}_z -sine modes. The cross-sectional profiles of the electric intensity distributions $|\mathcal{E}|^2$ of the fields in these normal modes are illustrated in Fig. 2 and are discussed in Sec. III.

B. Optical force between the nanofibers

A simple dispersion formula for the optical force between coupled parallel waveguides has been derived in Ref. [4]. According to Ref. [4], an adiabatic change in the separation

distance d shifts the eigenmode frequency ω and results in the optical force per unit length,

$$F = -\left(\frac{\partial U}{\partial d}\right)_\beta = -\frac{U}{\omega} \left(\frac{\partial \omega}{\partial d}\right)_\beta, \quad (1)$$

between the waveguides. Here, $U = N\hbar\omega$ is the energy per unit of propagation length of the field in an eigenmode of the combined system, with N being the corresponding number of photons. The derivative in Eq. (1) is taken at a fixed propagation constant β to ensure the translational invariance of the optical mode in the longitudinal direction. Negative and positive values of F correspond to attractive and repulsive forces.

Assume that the dispersion relation for the system is $\Phi(\omega, \beta, d) = 0$. The triple product (Euler's chain) rule reads $(\partial\omega/\partial\beta)_d(\partial\beta/\partial d)_\omega(\partial d/\partial\omega)_\beta = -1$. On the other hand, the optical power transmitted through the system is given as $P = v_g U$, where $v_g = (\partial\omega/\partial\beta)_d$ is the group velocity. Hence, Eq. (1) yields the dispersion formula [4]

$$F = \frac{P}{c} \left(\frac{\partial n_{\text{eff}}}{\partial d}\right)_\omega, \quad (2)$$

where $n_{\text{eff}} = \beta/k$ is the effective refractive index.

The optical force between the nanofibers can also be calculated from the Maxwell stress tensor. The components $T_{i'}$ with $i, i' = x, y, z$ of the cycle-averaged Maxwell stress tensor \mathbf{T} are given as [37]

$$T_{i'v} = \frac{1}{4} \text{Re}[\epsilon_0 n_{\text{ref}}^2 (2\mathcal{E}_i \mathcal{E}_{i'}^* - \delta_{i'v} |\mathcal{E}|^2) + \mu_0 (2\mathcal{H}_i \mathcal{H}_{i'}^* - \delta_{i'v} |\mathcal{H}|^2)], \quad (3)$$

where $n_{\text{ref}} = n_f$ inside a fiber and $n_{\text{ref}} = n_0$ outside the fibers. It is known that the cycle-averaged optical force \mathcal{F} on a body is [37]

$$\mathcal{F} = \oint_S \mathbf{T} \cdot d\mathbf{S}, \quad (4)$$

where S is a closed surface surrounding the body. We define \mathcal{F} as the optical force on nanofiber 2. The surface S for the integral in Eq. (4) for this force surrounds nanofiber 2, but not nanofiber 1. To calculate the surface integral, we choose an appropriate surface and take into account the fact that the amplitudes \mathcal{E} and \mathcal{H} of the electric and magnetic components of the field in the guided array mode quickly approach 0 in the limit $r \equiv \sqrt{x^2 + y^2} \rightarrow \infty$. We find that only the component \mathcal{F}_x of the force \mathcal{F} is nonzero. The optical force per unit length between the nanofibers is given by $F = \mathcal{F}_x/L$, where L is the length of the nanofibers. We get

$$F = - \int_{-\infty}^{\infty} T_{xx} dy, \quad (5)$$

where

$$T_{xx} = \frac{1}{4} [\epsilon_0 n_0^2 (2|\mathcal{E}_x|^2 - |\mathcal{E}|^2) + \mu_0 (2|\mathcal{H}_x|^2 - |\mathcal{H}|^2)] \quad (6)$$

and the integration is taken along the y axis (see Fig. 1). It has been shown for a variety of coupled systems that the results of the calculations for the force from Eq. (2) are identical to that of the calculations from Eq. (5) [4,8,9].

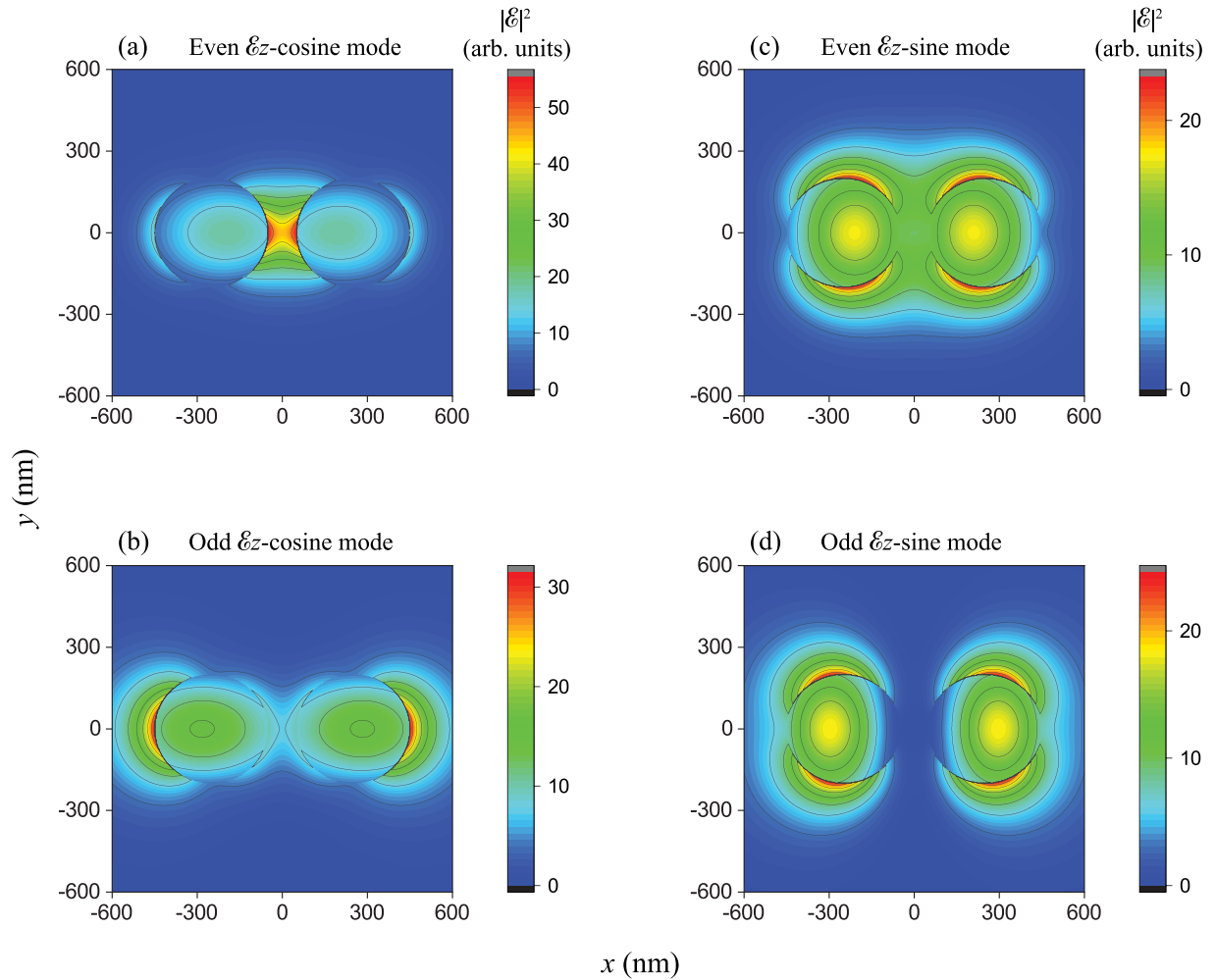


FIG. 2. Cross-sectional profiles of the electric intensity distributions $|\mathcal{E}|^2$ of the fields in (a) the even \mathcal{E}_z -cosine mode, (b) the odd \mathcal{E}_z -cosine mode, (c) the even \mathcal{E}_z -sine mode, and (d) the odd \mathcal{E}_z -sine mode of two identical parallel nanofibers. The fiber radius is $a = 200$ nm, the wavelength of light is $\lambda = 800$ nm, and the separation distance between the two fibers is $d = 100$ nm. The refractive index of the fibers is $n_f = 1.4533$ and that of the surrounding medium is $n_0 = 1$. The power of light is the same for the modes.

It is known that optical forces in waveguides can be generated not only by radiation pressure and the field gradient, but also by the electrostriction effect, which can create deformations of the waveguides [38]. Equations (2) and (5) describe only those optical forces that are produced by radiation pressure and the field gradient. In the present work, we neglect the electrostrictive forces, as in Refs. [4,8,9]. The electrostrictive forces scale to the fourth power of the material refractive index and can therefore be significant for a waveguide made of a high refractive index material, such as silicon [38]. On the other hand, the electrostrictive forces reduce with decreasing cross-sectional size of the waveguide [38]. Since the radius of a nanofiber is small and the refractive index of its silica core is not large (compared to that of silicon), we expect that the effects of the electrostrictive forces are not dramatic in the case of nanofibers.

III. NUMERICAL CALCULATIONS

In this section, we numerically calculate the optical force F produced by the field in a guided array mode of two identical

parallel vacuum-clad silica nanofibers. The refractive index of the vacuum cladding is, as already mentioned, $n_0 = 1$. To calculate the refractive index n_f of the silica cores of the nanofibers, the four-term Sellmeier formula for fused silica is used [39,40]. In particular, for light with the wavelength $\lambda = 800$ nm, we have $n_f = 1.4533$.

According to the previous section, in the case of identical fibers, there are four kinds of normal modes, denoted as the even \mathcal{E}_z -cosine, odd \mathcal{E}_z -cosine, even \mathcal{E}_z -sine, and odd \mathcal{E}_z -sine modes [27]. We are interested in the case where the fiber radius is small enough that no more than one normal mode of each kind can be supported by the fibers.

The spatial distributions of the fields in the guided array modes of two parallel fibers have been studied in Refs. [27,34]. In the present paper, we are interested in the optical forces between two nanofibers. These forces can be calculated from the gap-dependent effective refractive index n_{eff} (or the propagation constant β) for the array mode using Eq. (2). They can also be obtained from the field distributions using Eqs. (5) and (6).

We use the technique of Refs. [27,34] to calculate the field distributions of the guided array modes. In Fig. 2, we plot the cross-sectional profiles of the electric intensity distributions $|\mathcal{E}|^2$ of the fields in the even \mathcal{E}_z -cosine, odd \mathcal{E}_z -cosine, even \mathcal{E}_z -sine, and odd \mathcal{E}_z -sine modes. We see that $|\mathcal{E}|^2$ is symmetric with respect to the principal axes x and y . Figure 2(a) shows that the field intensity of the even \mathcal{E}_z -cosine mode is dominant in the area between the fibers. We observe from Fig. 2(b) that the field intensity of the odd \mathcal{E}_z -cosine mode is dominant in the outer vicinities of the left-side surface of the left-side fiber and the right-side surface of the right-side fiber. Figure 2(c) shows that the field intensity of the even \mathcal{E}_z -sine mode is dominant in the outer vicinities of the top and bottom parts of the surfaces of the fibers, and is significant in the area between the fiber surfaces. According to Fig. 2(d), the field intensity of the odd \mathcal{E}_z -sine mode is dominant in the vicinities of the top and bottom parts of the surfaces of the fibers, significant in the outer vicinities of the left-side surface of the left-side fiber and the right-side surface of the right-side fiber, and small in the area between the fibers.

It is clear from Fig. 2 that for each of the two interfacing nanofibers, the field intensity on the inward side (the right side of the left-side nanofiber or the left side of the right-side nanofiber) is different from the field intensity on the outward side (the left side of the left-side nanofiber or the right side of the right-side nanofiber). In the case of even array modes, the field intensity on the inward sides is stronger than that on the outward sides, while in the case of odd array modes, the relation is opposite. It is known that a polarizable microparticle with a dipole induced by a laterally varying optical field will be accelerated towards the region with a stronger field [41]. Nanofibers can be considered as a collection of microscopic dipolar subunits and, hence, can also be accelerated towards the regions with a stronger field. Consequently, we expect that the two nanofibers will be attracted toward or repulsed from each other by the field in an even or odd array mode, respectively.

We use the dispersion relation (2) to calculate the optical force F as functions of the fiber radius a , the light wavelength λ , and the separation distance d . We note that the use of expression (5) for F in terms of the Maxwell stress tensor gives the same numerical results (see Fig. 8).

We plot in Figs. 3 and 4 the power-normalized optical force per unit length, F/P , as functions of the fiber radius a and the light wavelength λ . The figures show that the magnitude of the optical force depends on the mode type and the sign of the force depends on the mode parity. Indeed, the forces of the even modes are negative (see the upper parts of the figures), while the forces of the odd modes are positive (see the lower parts of the figures). Thus, the optical forces between the nanofibers are attractive for the fields in the symmetric modes and repulsive for the fields in the antisymmetric modes, in agreement with the results for other systems of coupled waveguides and cavities [4–13]. These features are the consequences of the fact that for increasing fiber separation distance d , the propagation constant β and, hence, the effective refractive index $n_{\text{eff}} = \beta/k$ decrease in the case of the even array modes and increase in the case of the odd array modes [34]. The negative and positive signs of the optical forces are also in agreement with the field intensity distributions shown in

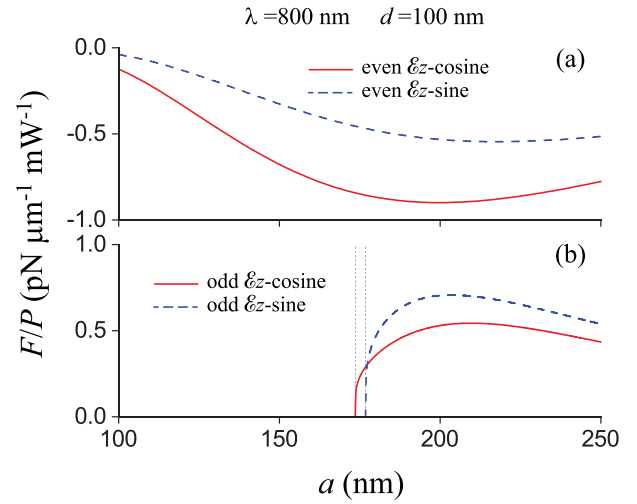


FIG. 3. Power-normalized optical force per unit length, F/P , as a function of the fiber radius a in the cases of (a) even and (b) odd array modes. The wavelength of light is $\lambda = 800$ nm and the separation distance between the two fibers is $d = 100$ nm. The refractive index of the fibers is $n_f = 1.4533$ and that of the surrounding medium is $n_0 = 1$. The vertical dotted lines indicate the positions of the cutoffs for the odd array modes.

Fig. 2, where the nanofibers are expected to be accelerated towards the regions with a stronger field. Note that the typical order of magnitude of the power-normalized force per unit length, F/P , for coupled nanofibers is $1 \text{ pN } \mu\text{m}^{-1} \text{ mW}^{-1}$, similar to that for coupled silicon strip waveguides [4], a silicon waveguide suspended over a silica substrate [8], and coupled silicon slab waveguides [9]. According to Ref. [4], the electrostatic force due to trapped or induced charges in

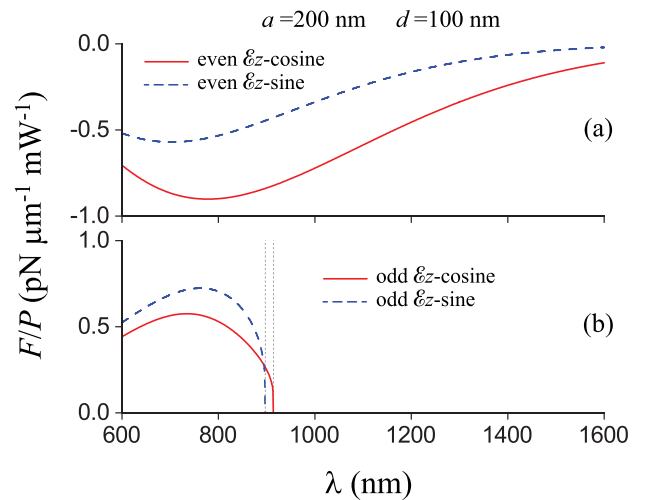


FIG. 4. Power-normalized optical force per unit length, F/P , as a function of the wavelength λ of light in the cases of (a) even and (b) odd array modes. The fiber radius is $a = 200$ nm and the separation distance between the two fibers is $d = 100$ nm. The refractive index n_f of the nanofibers is calculated from the four-term Sellmeier formula for fused silica [39,40] and that of the surrounding medium is $n_0 = 1$. The vertical dotted lines indicate the positions of the cutoffs for the odd array modes.

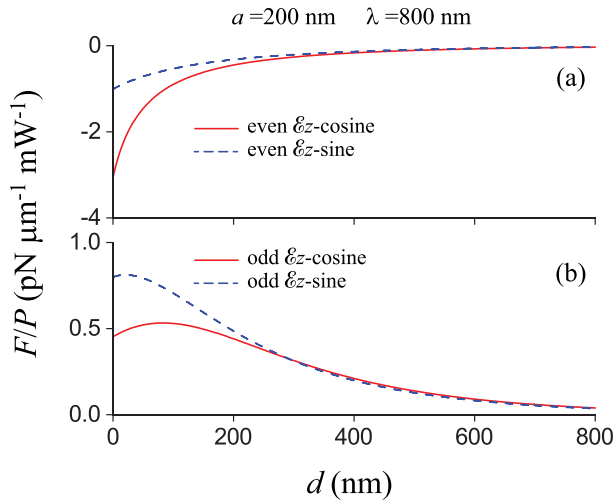


FIG. 5. Power-normalized optical force per unit length, F/P , as a function of the fiber separation distance d in the cases of (a) even and (b) odd array modes. The fiber radius and the light wavelength are $a = 200$ nm and $\lambda = 800$ nm, respectively. The refractive indices of the fibers and the surrounding medium are as in Fig. 3.

coupled silicon strip waveguides is at least one order smaller than the optical force, and the Casimir-Liftshitz is even smaller. We expect that similar relations between the forces can be realized in the case of nanofibers with an appropriate and reasonable power of light. We also note that for the power of 1 mW, the optical force between the nanofibers is about the same as the electrostatic force between nanomechanical optical fibers with integrated electrodes [42].

We observe from Figs. 3 and 4 that the odd \mathcal{E}_z -cosine and odd \mathcal{E}_z -sine modes have cutoffs, but the even \mathcal{E}_z -cosine and even \mathcal{E}_z -sine modes have no cutoff [27,33]. According to Ref. [34], the cutoff values of the fiber radius a and the light wavelength λ for the odd \mathcal{E}_z -cosine and \mathcal{E}_z -sine modes depend on the separation distance d between the two fibers. A smaller d leads to a larger cutoff value of the fiber radius a and to a smaller cutoff value of the light wavelength λ [34].

Figures 3 and 4 show that the dependencies of the power-normalized force F/P on the fiber radius a and the light wavelength λ are not monotonic: the absolute value $|F|/P$ of the power-normalized force has a local maximum as functions of a and λ . It is clear that when a is large enough or λ is small enough, the magnitude $|F|/P$ of the normalized force reduces with increasing a or decreasing λ . Similarly, when a is small enough or λ is large enough, the magnitude $|F|/P$ of the normalized force reduces with decreasing a or increasing λ in the case of even modes, or has a cutoff in the case of odd modes. Comparison between the solid red and dashed blue curves in Figs. 3(a) and 4(a) shows that the absolute value of the power-normalized force per unit length, F/P , for the even \mathcal{E}_z -cosine mode (solid red curves) is larger than that for the even \mathcal{E}_z -sine mode (dashed blue curves).

We plot, in Figs. 5–7, the power-normalized optical force per unit length, F/P , as a function of the fiber separation distance d for three different sets of values of the fiber radius a and the light wavelength λ . We observe from Fig. 5 that when the fiber radius a is large enough or, equivalently, the

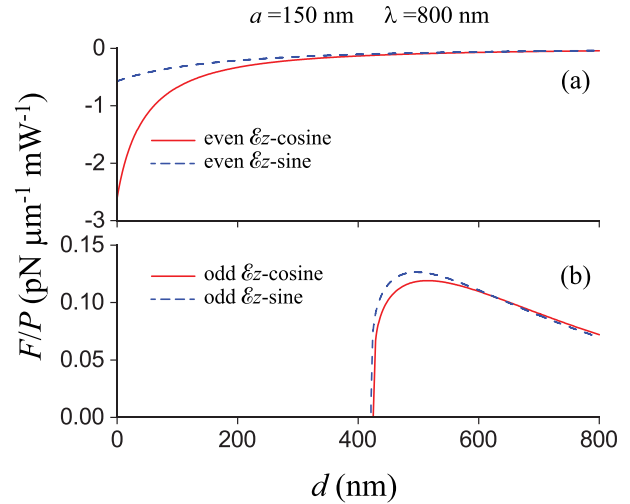


FIG. 6. Same as Fig. 5, except for $a = 150$ nm.

light wavelength is small enough, there is no cutoff of the guided normal modes for any separation distance d . However, Figs. 6(b) and 7(b) show that if the fiber radius a is small enough or, equivalently, the light wavelength is large enough, a cutoff of an odd guided normal mode may appear at a nonzero fiber separation distance d . We observe from Figs. 5–7 that the dependence of the normalized force F/P on the fiber separation distance d is monotonic for the even array modes, but not monotonic for the odd array modes.

Figures 5–7 show that the differences between the optical forces for the \mathcal{E}_z -cosine and \mathcal{E}_z -sine modes of the same even or odd parity reduce with increasing fiber separation distance d . This feature arises as a consequence of the fact that the differences between the optical forces for the \mathcal{E}_z -cosine and \mathcal{E}_z -sine array modes are determined by the differences between the propagation constants of the array modes and, hence, by the strength of the coupling between the nanofibers. This coupling depends on the mode overlap and hence reduces with increasing separation distance d . In addition, the dependence of the coupling on the mode polarization is very weak in the limit of large d [26,34].

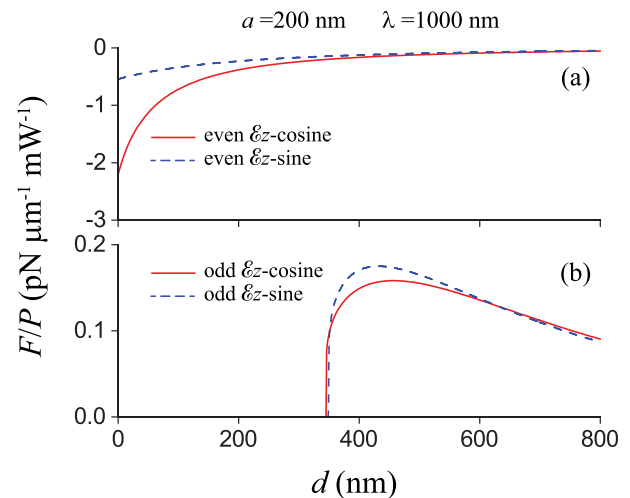


FIG. 7. Same as Fig. 5, except for $\lambda = 1000$ nm.

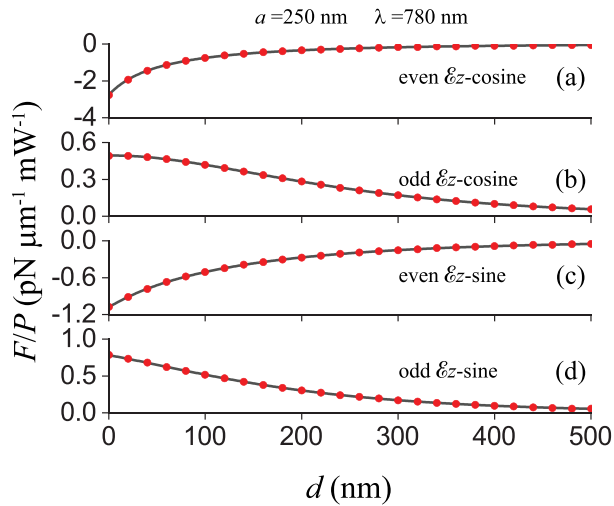


FIG. 8. Comparison between the results of the numerical calculations for the power-normalized optical force per unit length, F/P , using Eq. (2) (black lines) and Eq. (5) (red points). The fiber radius and the light wavelength are $a = 250$ nm and $\lambda = 780$ nm, respectively. The refractive indices of the fibers and the surrounding medium are as in Fig. 3.

We compare in Fig. 8 the results of the numerical calculations for the power-normalized optical force per unit length, F/P , using the dispersion relation (2) (black lines) and the Maxwell stress tensor relation (5) (red points). The figure shows that the two methods give the same numerical results for the optical force [4,8,9].

IV. SUMMARY

We have studied the optical force between two coupled identical parallel nanofibers using the rigorous array mode

theory. We have numerically demonstrated for the couple nanofibers that the forces of the even array modes are negative (attractive), while the forces of the odd array modes are positive (repulsive). We have investigated the dependencies of the optical forces on the array mode type, the fiber radius, the light wavelength, and the fiber separation distance. We have shown that the dependencies of the optical forces on the fiber radius and the light wavelength are, in general, nonmonotonic. For a given power and a given separation distance, the absolute value of the force achieves a peak when the fiber radius and the light wavelength are appropriate. Our results are important for controlling and manipulating the optical forces between coupled nanofibers.

The techniques used in this paper for the calculations of the optical force between two identical nanofibers can be extended to the case of two nonidentical nanofibers. Such an extension would require more extensive numerical calculations and a more comprehensive analysis for the normal array modes. Another possible extension is to consider the case where the field is in a superposition of an even mode and an odd mode. An appropriate manipulation of the superposition may result in a trapping potential for the nanofibers. Due to the complexity and rich underlying physics, the aforementioned potential extensions deserve to be studied separately in future work.

ACKNOWLEDGMENTS

This work was supported by the Okinawa Institute of Science and Technology (OIST) Graduate University and by the Japan Society for the Promotion of Science (JSPS) Grant-in-Aid for Scientific Research (C) under Grants No. 19K05316 and No. 20K03795. S.N.C. acknowledges support by Investments for the Future from LabEx PALM (Grant No. ANR-10-LABX-0039-PALM). The authors gratefully acknowledge J. Twamley for useful discussions.

-
- [1] A. W. Snyder and J. D. Love, *Optical Waveguide Theory* (Chapman and Hall, London, 1983).
 - [2] D. Marcuse, *Light Transmission Optics* (Krieger, Malabar, FL, 1989).
 - [3] K. Okamoto, *Fundamentals of Optical Waveguides* (Elsevier, New York, 2006).
 - [4] M. L. Povinelli, M. Lončar, M. Ibanescu, E. J. Smythe, S. G. Johnson, F. Capasso, and J. D. Joannopoulos, Evanescent-wave bonding between optical waveguides, *Opt. Lett.* **30**, 3042 (2005).
 - [5] P. T. Rakich, M. A. Popović, and Z. Wang, General treatment of optical forces and potentials in mechanically variable photonic systems, *Opt. Express* **17**, 18116 (2009).
 - [6] D. van Thourhout and J. Roels, Optomechanical device actuation through the optical gradient force, *Nat. Photon.* **4**, 211 (2010).
 - [7] A. W. Rodriguez, P.-C. Hui, D. N. Woolf, S. G. Johnson, M. Lončar, and F. Capasso, Classical and fluctuation-induced electromagnetic interactions in micron-scale systems: designer bonding, antibonding, and Casimir forces, *Ann. Phys. (Berlin)* **527**, 45 (2015).
 - [8] J. R. Rodrigues and V. R. Almeida, Optical forces through the effective refractive index, *Opt. Lett.* **42**, 4371 (2017).
 - [9] M. A. Miri, M. Cotrufo, and A. Alu, Optical gradient forces between evanescently coupled waveguides, *Opt. Lett.* **43**, 4104 (2018).
 - [10] J. Ng, C. T. Chan, P. Sheng, and Z. F. Lin, Strong optical force induced by morphology-dependent resonances, *Opt. Lett.* **30**, 1956 (2005).
 - [11] M. L. Povinelli, S. G. Johnson, M. Lončar, M. Ibanescu, E. J. Smythe, F. Capasso, and J. D. Joannopoulos, High- Q enhancement of attractive and repulsive optical forces between coupled whispering-gallery-mode resonators, *Opt. Express* **13**, 8286 (2005).
 - [12] A. Mizrahi and L. Schächter, Mirror manipulation by attractive and repulsive forces of guided waves, *Opt. Express* **13**, 9804 (2005).
 - [13] P. T. Rakich, M. A. Popovic, M. Soljagic, and E. P. Ippen, Trapping, corralling and spectral bonding of optical resonances through optically induced potentials, *Nat. Photon.* **1**, 658 (2007).

- [14] M. Eichenfield, C. P. Michel, R. Perahia, and O. Painter, Actuation of micro-optomechanical systems via cavity-enhanced optical dipole forces, *Nat. Photon.* **1**, 416 (2007).
- [15] M. Li, W. H. P. Pernice, C. Xiong, T. Baehr-Jones, M. Hochberg, and H. X. Tang, Harnessing optical forces in integrated photonic circuits, *Nature (London)* **456**, 480 (2008).
- [16] M. Li, W. H. P. Pernice, and H. X. Tang, Tunable bipolar optical interactions between guided lightwaves, *Nat. Photon.* **3**, 464 (2009).
- [17] J. Roels, I. De Vlaminck, L. Lagae, B. Maes, D. Van Thourhout, and R. Baets, Tunable optical forces between nanophotonic waveguides, *Nat. Nanotechnol.* **4**, 510 (2009).
- [18] G. S. Wiederhecker, L. Chen, A. Gondarenko, and M. Lipson, Controlling photonic structures using optical forces, *Nature (London)* **462**, 633 (2009).
- [19] T. A. Birks, D. O. Culverhouse, S. G. Farwell, and P. St. J. Russell, All-fiber polarizer based on a null taper coupler, *Opt. Lett.* **20**, 1371 (1995).
- [20] C. Ding, V. Loo, S. Pigeon, R. Gautier, M. Joos, E. Wu, E. Giacobino, A. Bramati, and Q. Glorieux, Fabrication and characterization of optical nanofiber interferometer and resonator for the visible range, *New J. Phys.* **21**, 073060 (2019).
- [21] L. Shao, Y. Xu, H. Wu, W. Fang, and L. Tong, Experimental demonstration of a compact variable single-mode fiber coupler based on microfiber, *IEEE Photon. Technol. Lett.* **33**, 687 (2021).
- [22] L. Tong, R. R. Gattass, J. B. Ashcom, S. He, J. Lou, M. Shen, I. Maxwell, and E. Mazur, Subwavelength-diameter silica wires for low-loss optical wave guiding, *Nature (London)* **426**, 816 (2003).
- [23] T. Nieddu, V. Gokhroo, and S. Nic Chormaic, Optical nanofibres and neutral atoms, *J. Opt.* **18**, 053001 (2016).
- [24] P. Solano, J. A. Grover, J. E. Homan, S. Ravets, F. K. Fatemi, L. A. Orozco, and S. L. Rolston, Optical nanofibers: A new platform for quantum optics, *Adv. At. Mol. Opt. Phys.* **66**, 439 (2017).
- [25] K. Nayak, M. Sadgrove, R. Yalla, F. Le Kien, and K. Hakuta, Nanofiber quantum photonics, *J. Opt.* **20**, 073001 (2018).
- [26] F. Le Kien, L. Ruks, S. Nic Chormaic, and T. Busch, Coupling between guided modes of two parallel nanofibers, *New J. Phys.* **22**, 123007 (2020).
- [27] W. Wijngaard, Guided normal modes of two parallel circular dielectric rods, *J. Opt. Soc. Am.* **63**, 944 (1973).
- [28] E. Yamashita, S. Ozeki, and K. Atsuki, Modal analysis method for optical fibers with symmetrically distributed multiple cores, *J. Lightwave Technol.* **3**, 341 (1985).
- [29] N. Kishi, E. Yamashita, and H. Kawabata, Modal and coupling-field analysis of optical fibers with linearly distributed multiple cores, *J. Lightwave Technol.* **7**, 902 (1989).
- [30] H. S. Huang and H. C. Chang, Analysis of equilateral three-core fibers by circular harmonics expansion method, *J. Lightwave Technol.* **8**, 945 (1990).
- [31] C. S. Chang and H. C. Chang, Vector normal modes on two-core optical fibers. I. The normal mode solutions, *J. Lightwave Technol.* **15**, 1213 (1997).
- [32] H. S. Huang and H. C. Chang, Vector coupled-mode analysis of coupling between two identical optical fiber cores, *Opt. Lett.* **14**, 90 (1989).
- [33] C. S. Chang and H. C. Chang, Vector normal modes on two-core optical fibers. II. The modal cutoffs, *J. Lightwave Technol.* **15**, 1225 (1997).
- [34] F. Le Kien, L. Ruks, S. Nic Chormaic, and T. Busch, Spatial distributions of the fields in guided normal modes of two coupled parallel optical nanofibers, *New J. Phys.* **23**, 043006 (2021).
- [35] F. Le Kien, S. Nic Chormaic, and T. Busch, Optical trap for an atom around the midpoint between two coupled identical parallel optical nanofibers, *Phys. Rev. A* **103**, 063106 (2021).
- [36] L. Shao, H. Wu, W. Fang, and L. Tong, Twin-nanofiber structure for a highly efficient single-photon collection, *Opt. Express* **30**, 9147 (2022).
- [37] J. D. Jackson, *Classical Electrodynamics* (Wiley, New York, 1998).
- [38] P. T. Rakich, P. Davids, and Z. Wang, Tailoring optical forces in waveguides through radiation pressure and electrostrictive forces, *Opt. Express* **18**, 14439 (2010).
- [39] I. H. Malitson, Interspecimen comparison of the refractive index of fused silica, *J. Opt. Soc. Am.* **55**, 1205 (1965).
- [40] G. Ghosh, *Handbook of Thermo-Optic Coefficients of Optical Materials with Applications* (Academic Press, San Diego, 1997).
- [41] H. C. van de Hulst, *Light Scattering by Small Particles* (Dover, Mineola, NY, 1981).
- [42] N. Podoliak, Z. Lian, M. Segura, W. H. Loh, and P. Horak, Electrostatic actuation of nanomechanical optical fibers with integrated electrodes (unpublished).